ЕФИ-731(46)-84

ЦЕНТРАЛЬНЫЙ НАУЧНО-ИССЛЕДОВАТЕЛЬСКИЙ ИНСТИТУТ
ИНФОРМАЦИИ И ТЕХНИКО-ЭКОНОМИЧЕСКИХ ИССЛЕДОВАНИЙ
ПО АТОМНОЙ НАУКЕ И ТЕХНИКЕ

A.S.BAGDASARYAN, S.V.ESAYBEGYAN, N.L.TER-ISAAKYAN

# FORMFACTORS OF MESONS AND MESON RESONANCES AT SMALL AND INTERMEDIATE MOMENTUM TRANSFERS $Q^2$ IN THE RELATIVISTIC QUARK MODEL

ЕРЕВАН-1984

ЕФИ-731(46)-84

А.С.БАГДАСАРЯН, С.В.ЕСАЙБЕГЯН, Н.Л.ТЕР-ИСААКЯН

# ФОРМФАКТОРЫ МЕЗОНОВ И МЕЗОННЫХ РЕЗОНАНСОВ ПРИ МАЛЫХ И ПРОМЕЖУТОЧНЫХ ПЕРЕДАЧАХ $Q^2$ В РЕЛЯТИВИСТСКОЙ КВАРКОВОЙ МОДЕЛИ

В релятивистской кварковой модели исследована структура волновой функции пиона и получены предсказания для формфакторов $\pi$ , $\rho$ , $A_1$ , - мезонов и формфакторов $\omega \to \pi\gamma$ и $A_1 \to \pi\gamma$ переходов. Результаты для формфакторов $\pi$ , $A_1$ , - мезонов, $\omega \to \pi\gamma$ перехода, и формфактора $G_2$ $A_1 \to \pi\gamma$ перехода находятся в хорошем количественном согласии с предсказаниями дисперсионных правил сумм КХД. Результаты по формфакторам $\rho$ - - мезона превышают предсказания правил сумм КХД примерно в 2 раза.

Ереванский физический институт
Ереван 1984

ЕФИ-731(46)-84

A.S.BAGDASARYAN, S.V.ESAYSEGYAN, N.L.TER-ISAAKYAN

# FORMFACTORS OF MESONS AND MESON RESONANCES AT SMALL AND INTERMEDIATE MOMETUM TRANSFERS $Q^2$ IN THE RELATIVISTIC QUARK MODEL

The structure of the pion wave function is investigated in the relativistic quark model as well as the predictiors for the formfactors of both $\pi$ , $\rho$ , $A_1$ -mesons $\omega \to \pi\gamma$ and $A_1 \to \pi\gamma$ transitions are obtained. The results for the formfactors of $\pi$ . $A_1$ -mesons. $\omega \to \pi\gamma$ transition and the formfactor $G_2$ of $A_1 \to \pi\gamma$ transition are in good qualitative agreement with the QCD dispersion sum rule predictions. The results for the $\rho$ -meson formfactors approximately twice as much exceed the predictions of the QCD sum rules.

Yerevan Physics Institute

Yerevan 1984

## 1. Introduction

As is well known, the QCD perturbation theory describes well the strong interaction physics at short distances. With the increase of distances the non-perturbative effects become essential. At present, these effects can be taken into account semi-phenomenologically, on the basis of the QCD dispersion sum rules (DSR) method (see, e.g. [1]).

On the other hand, as follows from the analysis of the low-energy experimental data, in the region of relatively large distances takes place a simple physical picture in which hadron is represented as a bound state of the relativistic constituent quarks. The phenomenological model based on such representation [2,6] enabled one to describe self-consistently a number of the low-energy characteristics of hadrons: the magnetic moments and electromagnetic radii of the nucleons [5,6], the magnetic moments and leptonic decays of the baryon octet [7], the radiative decays of the baryon resonances [8]. In the framework of the model a consistent description of the meson static characteristics and available data on $\pi$ -meson formfactors were also obtained [9].

Emphasize that QCD sum rules method and relativistic quark model (RQM in what follows) pretend to describe the same region of hadronic physics

and lead mainly to the similar results, although sometimes there arise essential differences, e.g. in the investigation of the structure of the pion wave function axial projection [9,10].

In order to clarify a closer connection between the both approaches, it is reasonable to consider within RQM some formfactors of mesons and meson resonances which have been calculated by the QCD sum rule method [11-14]. This problem is interesting also from the viewpoint of clarifying the dependence of these quantities on the quantum numbers.

## 2. Low-Energy Characteristics and Structure of meson Wave Functions

Some results of this Section were obtained earlier, so we give them for completeness. We proceed from the formulation of the relativistic quark model in the infinite momentum frame (IMF) [5,6], which is based on the consideration of the time-ordered diagrams of the old-fashioned perturbation theory.

The vertex functions of $\pi^+$, $\rho^+(\omega)$ and $A_1$-mesons have the following

$$\pi^+ = \frac{\delta_{ij}\,\Psi_\pi(P_1,P_2)}{\sqrt{6}\;2M_0^2(M_0+2m)}\;\bar{U}^i_u(P_1)(\hat{P}_0+M_0)\gamma_5(-\hat{P}_2+M_0)V^j_{\bar{d}}(-P_2)$$

$$\rho^+(\omega) = \frac{\delta_{ij}\,\Psi_\rho(P_1,P_2)}{\sqrt{6}\;2M_0^2(M_0+2m)}\;\bar{U}^i_u(P_1)(\hat{P}_0+M_0)\gamma_\mu(-\hat{P}_2+M_0)V^j_{\bar{d}}(-P_2)\;e^s_\mu(P_0) \qquad (2)$$

$$A_1(a_1) = \frac{\delta_{ij}\,\Psi_{A_1}(P_1,P_2)}{\sqrt{6}\;2M_0^2(M_0+2m)}\;\bar{U}^i_u(P_1)(\hat{P}_0+M_0)\gamma_\mu(-\hat{P}_2+M_0)V^j_{\bar{d}}(-P_2)\;\frac{\epsilon_{\mu\rho\alpha\lambda}}{M_0^2}\cdot$$

(3)

$$P_{0\rho}A_\rho\,e^s_\lambda(P_0) \equiv \frac{\delta_{ij}\,\Psi_{A_1}(P_1,P_2)}{\sqrt{6}\;M_0}\;\bar{U}^i_u(P_1)\gamma_\mu\gamma_5 V^j_{\bar{d}}(-P_2)\,e^s_\mu(P_0)$$

Here $P_1$ and $P_2$ are 4-momenta of $u, \bar{d}$ -quarks; $P_0 = P_1 + P_2$, $A = P_1 - P_2$, $m$ is the mass of $u$ and $d$ -quarks; $M_0^2 = P_0^2$ is the invariant mass of the system of quarks composing meson; $i, j$ are color indices, $e_\mu^s(P_0)$ are the polarization vectors of $\rho$ and $A_1$ mesons. Radial part of the vertex functions $\Psi_{\pi(\rho, A_1)}$ describes the momentum distribution of quarks in meson. Vertex functions (1-3) expressed via Pauli spinors in the rest frame $\vec{P}_0 = 0$ have a standard SU(6) structure.

When considering the electromagnetic transitions $B \to B' + \gamma^*$, it is necessary to use the IMF in which $q_0 = -q_3 = \frac{M^2 - M'^2 - q_\perp^2}{4P}$, $q^2 = -q_\perp^2$ [5,6]. For the initial quark momenta we have a parametrization at $P \to \infty$.

$$\vec{P}_i = x_i \vec{P} + \vec{K}_{\perp i}; \quad \sum \vec{K}_\perp^i = 0 \qquad \sum x_i = 1 \tag{4}$$

We assume that the photon interacts with a first quark and for the final quark momentum we have

$$\vec{K}'_{1\perp} = \vec{K}_{1\perp} - x_2 \vec{q}_\perp \tag{5}$$
$$\vec{K}'_{2\perp} = \vec{K}_{2\perp} + x_2 \vec{q}_\perp$$

Invariant masses of the systems of initial and final quarks are equal to

$$M_0^2 = \frac{K_\perp^2 + m^2}{x_1 x_2}, \quad \vec{K}_{1\perp} = \vec{K}_\perp; \quad M_0'^2 = \frac{K_\perp'^2 + m^2}{x_1 x_2}, \quad \vec{K}'_{\perp 1} = \vec{K}'_\perp \tag{6}$$

The parameter $x_i$ is connected with the quark momenta in the frame $\vec{P}_0 = 0$ $K_i(\omega, K_i)$

$$x_i = \frac{\omega_i + K_{iz}}{2\omega_i} \qquad \omega_i = \frac{M_0}{2} = \sqrt{\vec{K}^2 + m^2} \tag{7}$$

Vertex functions (1-3) in the frame $P_0 \to \infty$ if expressed via two-component spinors

$$W_n = \sum W_m U_{mn}(K_i) \tag{8}$$

where

$$U(K_i) = \frac{m + \omega_i + K_{iz} + i\,\epsilon_{mn}\,6_m\,K_{in}}{[K_{i\perp}^2 + (m + \omega_i + K_{iz})^2]^{1/2}} \qquad i = 1, 2 \qquad (9)$$

have the same structure as in the frame $P_o = 0$ [5,6].

In accordance with the results of [2-4] we assume that the radial part of the vertex function $\Psi(P_1, P_2)$, at least in the characteristic region of the variable variation can be considered as a function of one variable $M_o^2$. To achieve a complete analogy with the works [3,4] we introduce the notations

$$\Phi(M_o^2) = \Psi(P_1, P_2) \big/ M^2 - M_o^2 \qquad (10)$$

where $M$ is the meson mass, the denominator $M^2 - M_o^2$ naturally arises in the old-fashioned perturbation theory in IMF (for details, see Ref.[6]). The function $\Phi(M_o^2)$ corresponds to the radial wave function of Refs.[2-4].

We assume the exponential form of the wave function $\Phi(M_o^2)$

$$\Phi(M_o^2) = \frac{\pi N}{\Lambda^2} M_o\, e^{-M_o^2/4\Lambda^2} \quad *) \qquad (11)$$

where $N$ is the normalization parameter. The wave function $\Phi(M_o^2)$ depends on two quantities: the constituent quark mass $m$ and parameter $\Lambda^2$ which determines characteristic momenta of quarks in the meson $\langle K^2 \rangle \sim \Lambda^2$ which, generally speaking, may be different for $\pi$, $\rho$ and $A_1$ mesons.

Parameters $m^2$ and $\Lambda^2$ can be found from the description of the meson

---

*) The introduction of factor $M_o$ is not essential. At such parametrization the formulae for some formfactors become simpler. In Refs.[2,3]

$$\Phi(M_o^2) = N\sqrt{\frac{M_o}{2\pi}}\, e^{-M_o^2/\Lambda^2}$$

low-energy characteristics: $f_\pi$ (the constant of $\pi \to \mu\nu$ decay), $f_\rho$ (the constant of $\rho \to \gamma$ transition), $f_{\omega\pi}$ (the amplitude of $\omega \to \pi\gamma$ decay) and $r_\pi^2$ ( mean-square radius of pion). There are no experimental data in the case of $A_1$ -meson. We shall define the unknown parameter $\Lambda_{A_1}$ from the description of quantity $f_A$

$$\langle 0 | J_\mu^A(0) | A_1(P,\lambda) \rangle = f_A e_\mu^\lambda(P) \tag{12}$$

where $J_\mu^A = \bar{\Psi}_u \gamma_\mu \gamma_5 \Psi_d$ is axial current, whose value $f_A = 0.21$ GeV$^2$ has been obtained by QCD sum rules method [15].

The quantities $f_\pi$ , $f_\rho$ , $f_{\omega\pi}$ and $\langle r_\pi^2 \rangle$ were originally considered in the light front formulation of relativistic quark model in Ref.[3] (see also [10] ). In the diagram formulation of the model these quantities can be calculated on the basis of the corresponding graphs of the old-fashioned perturbation theory in IMF (Fig.1). The results are given in our previous work [9] . A good description of data on $f_\pi$ , $f_\rho$ , $f_{\omega\pi}$ and $\langle r_\pi^2 \rangle$ was obtained at the following values of the parameters

$$m = 0.260 \text{ GeV}; \qquad \Lambda_\pi = \Lambda_\rho = \Lambda_u = 0.415 \text{ GeV} \tag{13}$$

For the quantity $f_A$ we obtained the expression

$$f_A = \frac{4\sqrt{6}\,\Lambda_A^2\, N_A}{\pi} \int_0^1 x_1 x_2\, e^{-m^2/4\Lambda_A^2 x_1 x_2}\, dx_1 \tag{14}$$

At $\Lambda_A = 0.415$ GeV $f_A = 0.215$ GeV$^2$ what is in good agreement with the result of QCD sum rules.

Thus, the quark-meson vertices being chosen as (1-3), the low-energy parameters of mesons can be described at $\Phi_\pi(M_0^2) = \Phi_\rho(M_0^2) = \Phi_\omega(M_0^2) = \Phi_{A_1}(M_0^2)$ , i.e. the SU(6) symmetry relation takes place

for the vertex functions*).

The value of the parameter $\Lambda = 0.415$ GeV corresponds to the following values of mean-square quark momenta: $\frac{\langle k^2 \rangle}{m^2} \simeq 2,3$ in $\pi$, $\rho$, $\omega$ mesons and $\frac{k^2}{m^2} \simeq 2,7$ in $A_1$ meson, i.e. the quarks in the mesons must be strongly relativistic.

Turn now to the investigation of the structure of the pion wave function. Consider the matrix elements of the bilocal operators:

$$\langle 0 | J^A_\mu(z_1 - z) | \pi(P) \rangle = i \left( P_\mu \varphi^\pi_A(2zP) + 2z_\mu \tilde{\varphi}_A(2zP) \right) \qquad (15)$$

$$\varphi^\pi_A(0) = f^\pi_A = f_\pi \qquad \tilde{\varphi}^\pi_A(0) = \tilde{f}_A$$

$$\langle 0 | J^P(z_1 - z) | \pi(P) \rangle = \varphi^\pi_P(2zP) \qquad (16)$$

$$\varphi^\pi_P(0) = f^\pi_P$$

$$\langle 0 | J^T_{\mu\nu}(z_1 - z) | \pi(P) \rangle = 2\epsilon_{\mu\nu\alpha\beta} P_\alpha z_\beta \varphi^\pi_T(2zP) \qquad (17)$$

$$\varphi^\pi_T(0) = f^\pi_T$$

where $J^A_\mu(z_1 - z) = \bar{\Psi}_d(z) \gamma_\mu \gamma_5 \Psi_u(-z)$, $J^P(z_1 - z) = i \bar{\Psi}_d(z) \gamma_5 \Psi_u(-z)$

$J^T_{\mu\nu}(z_1 - z) = i \bar{\Psi}_d(z) \sigma_{\mu\nu} \Psi_u(-z)$ at $z^2 \to 0$

which define the axial, pseudoscalar and tensor projections of the pion wave function (see, e.g. [12]).

---

*) Emphasize that the experimental data allow the relation $\Lambda_\pi = \Lambda_\rho = \Lambda_\omega$, but the latter does not follow from them. A good description of the data is possible, in principle, also at $\Lambda_\pi \neq \Lambda_\rho$ [9].

$$\varphi_I^{\pi}(x) = \frac{1}{2P_{\pi}} \int e^{-i z P \xi} \varphi_I(zP) \, d(zP) \qquad (18)$$

$$f_I = 2 \int_0^1 \varphi_I(x)\, dx$$

where $\xi = 1-2x$, $I = A, P, T$. The axial projection of $\varphi_A^{\pi}(x)$ defines the pion formfactor asymptotics in the perturbative QCD, the pseudoscalar and tensor projections define the power corrections to the asymptotics (the terms $\sim \frac{1}{Q^4}$) [16]. Of particular interest is the matrix element (16) since the constant $f_P^{\pi}$ may be related to the current masses of $u$ - and $d$-quarks $f_P = \frac{m_{\pi}^2}{\mu_u + \mu_d} f_{\pi}$

In the framework of the model, the matrix elements (15-17) can be easily calculated using non-covariant perturbation theory graphs (Fig.1c, where a cross denotes a corresponding bilocal operator).

We have received the following expressions for the wave functions:

$$\varphi_A^{\pi}(x) = \frac{\sqrt{3}\, m}{16 P_{\pi}^2 \sqrt{2}\, x(1-x)} \int_0^{\infty} \Phi(M_0^2)\, d\kappa_{\perp}^2 = \frac{\sqrt{3}\, m N_{\pi}}{2\sqrt{2} P_{\pi}} e^{-\frac{m^2}{4\Lambda^2 x(1-x)}} \qquad (19)$$

$$f_{\pi} = 0{,}133\ \text{ГэВ} \; ; \quad \tilde{\varphi}_A(x) \equiv 0$$

$$\varphi_P^{\pi}(x) = \frac{\sqrt{3}}{32 P_{\pi}^2 \sqrt{2} x(1-x)} \int_0^{\infty} M_0^2 \Phi(M_0^2)\, d\kappa_{\perp}^2 =$$

$$\frac{\sqrt{3} m^2 N_{\pi}}{4 P_{\pi} \sqrt{2}} \left( \frac{4\Lambda^2}{m^2} + \frac{1}{x(1-x)} \right) e^{-\frac{m^2}{4\Lambda^2 x(1-x)}} \qquad (20)$$

$$f_P = 0{,}273\ (\text{ГэВ})^2$$

$$\varphi_T^{\pi}(x) = -\frac{\sqrt{3}}{32 P_{\pi}^2 \sqrt{2}\, x(1-x)} \int_0^{\infty} \kappa_{\perp}^2 \Phi(M_0^2)\, d\kappa_{\perp}^2 = -\frac{\sqrt{3}\Lambda^2 N_{\pi}}{\sqrt{2} P_{\pi}} \cdot \qquad (21)$$

$$\cdot x(1-x) e^{-m^2/4\Lambda^2 x(1-x)}$$

$$f_T = -0{,}0343\ (\text{ГэВ})^2$$

The obtained value of the pseudoscalar constant $f_P$ corresponds to the value of $\mu_u + \mu_d = 9.4$ MeV, thus being in good agreement with the experiment (see also [10] ). Note also an interesting relation between the constants $f_\pi$ , $f_P$ and $f_T$

$$f_P = -6 f_T + 2m f_\pi \tag{22}$$

which takes place irrespective of the form of the vertex function $\Phi(M_0^2)$ .

The normalized wave functions $2\varphi_I(x)/f_I$ together with the asymptotic wave function $\varphi_A(x) = 3 f_\pi x(1-x)$ are given in Fig.2. Note that the wave function $\varphi_A^\pi(x)$ is close to the asymptotic one and essentially differs from that obtained in [17] by QCD sum rules method. A detailed investigation of the properties of the meson wave functions (including the strange and charmed mesons) as well as a comparison with the DSR results will be carried out in a separate work. In this paper, in addition to the pion wave functions (19-21) we shall present only the vector projections of the $\rho$ -meson wave function for longitudinal and transverse polarizations, respectively:

$$\varphi_\rho^{\parallel} = \frac{\sqrt{3}}{32\pi^2 x(1-x)\sqrt{2}} \int_0^\infty \Phi(M_0^2)\left(M_0 - \frac{4K_3^2}{M_0+2m}\right) dK_\perp^2 \tag{23}$$

$$\varphi_\rho^{\perp} = \frac{\sqrt{3}}{32\pi^2 x(1-x)\sqrt{2}} \int_0^\infty \Phi(M_0^2)\left(M_0 - \frac{2K_\perp^2}{M_0+2m}\right) dK_\perp^2 \tag{24}$$

$$2\int_0^1 \varphi_\rho^{\parallel}(x)\,dx = 2\int_0^1 \varphi_\rho^{\perp}(x)\,dx = f_\rho \tag{25}$$

The function $\varphi_\rho^{\parallel}(x)$ determines the $\rho$ -meson formfactor asymptotics in QCD (see, e.g. [16] ). It is interesting to note the essential dependence of the $\rho$ -meson wave function on its polarization. The function $\varphi_\rho^{\perp}(x)$ turned out to be considerably broader than $\varphi_\rho^{\parallel}(x)$ . We do not give the

curves for these functions, since $\varphi_\rho^{''}(x)/f_\rho$ is close to $\varphi_{A}^{ac}(x)/f_{\pi}$, and $\varphi_\rho^{\perp}(x)/f_\rho$ practically coincides with $\varphi_\rho^{\pi}(x)/f_\rho$.

3. Formfactors of $\pi$, $\rho$ and $A_1$ Mesons.

1) Formfactor of pion. As was already mentioned in a series of works [9, 11-13], in the region of not too large momentum transfers $Q^2$ the behaviour of the electromagnetic formfactors is not connected to the QCD perturbation theory and is determined by the non-perturbative effects. In our previous work [9] it was in particular shown, that the pion electromagnetic formfactor can be described up to $Q^2 \sim 5\ (\text{GeV})^2$ in the relativistic quark model on the basis of a simplest quark diagram without gluon exchange (Fig.3), whereas the contribution of perturbative effects in this region does not exceed 30%. The formulae for the meson electromagnetic formfactors in RQM have a similar structure, therefore, in this Section we shall restrict ourselves to a detailed investigation of the pion formfactor [3,9]

$$F^{\pi}(Q^2) = \frac{m^2 N^2}{8\Lambda^2} \int_0^1 \exp\left\{-\frac{m^2 + \frac{q_\perp^2}{4}(1-x)^2}{2\Lambda^2 x(1-x)}\right\} \cdot \left[1 - \frac{q_\perp^2 (1-x)^2}{4m^2} + \frac{2\Lambda^2 x(1-x)}{m^2}\right] \frac{dx}{x(1-x)} \tag{26}$$

As one can see from Fig.3, the formula (26) describes well the experimental data up to $Q^2 \sim 5\ (\text{GeV})^2$, while at large $Q^2$ the curve falls off more rapidly. It is interesting that in this region the results depend weakly on the form of the vertex function and the formfactor falls off approximately in a power-law way. This fact was originally mentioned in Ref.[8]. Let us explain it at greater length. According to the 4-momentum conservation law in IMF, the momentum transfer $q_\perp$ is always present in the combination $q_\perp^2 (1-x)^2/4$, i.e. the $Q^2$ dependence is strongly weakened. In the

region $0.1 < x < 0.9$ the function $\exp\left[-\frac{m^2}{2\Lambda^2 x(1-x)}\right]$ is close to $x(1-x)$ ; therefore at $q_\perp^2 \lesssim 8\Lambda^2$ the main contribution to the integral comes from the range $(1-x) \lesssim 8\Lambda^2/q_\perp^2$ , hence we have approximately power behaviour of formfactor $F \sim 1/q_\perp^2$ . At further increase of $q_\perp^2$ the values of $(1-x) \sim \frac{1}{q_\perp}$ become essential, so the power-law behaviour of the formfactor transforms gradually into the exponential behaviour of the type of $e^{-\beta q_\perp}$ .

One should however mind that the constituent quark mass is an effective parameter which should depend on characteristic distances in hadron which apparently decrease as $Q^2$ grows. Therefore in the region of large momentum transfers it is wrong to regard the quark mass constant. It is natural to take the quantity $1/M_0^2$ as invariant measure of characteristic distances in hadron, hence $m = m(M_0^2)$ (see also [3] ). If we assume that the constituent quark mass is determined mainly by the vacuum expectation value $\langle 0|\bar{\Psi}\Psi|0\rangle$ (see, e.g. [18] ), then following the dimensionality considerations we have $m \sim \frac{\langle 0|\bar{\Psi}\Psi|0\rangle}{M_0^2}$ at large $M_0^2$ . Under such assumption, the values of $1-x \sim q_\perp^{-3/2}$, $M_0^2 \sim (1-x)^{-1/3} \sim \sqrt{q_\perp}$, $m^2 \sim (1-x)^{2/3} \sim q_\perp^{-1}$ are essential in the integral (26) at $q_\perp^2 > 8\Lambda^2$ . From here it follows, in particular, that $q_\perp$ dependence in (26) is strongly smoothened, the quark mass falls off very slowly with increase of $q_\perp$ and cannot be neglected even at very large $q_\perp^2$ $(q_\perp^2 (1-x)^2 \sim m^2)$

Emphasize, that the experimental data also indicate the slow dependence of $m(q_\perp^2)$ at least up to $q_\perp^2 \sim 5$ GeV$^2$, because formula (26) with constant mass "works" well in this region.

Hereafter we shall admit for $m(q_\perp^2)$ the following formula

$$m^2(Q^2) = \frac{m^2}{(1 + Q^2/Q_0^2)^{1/2}} \qquad (27)$$

where $m = 0.26$ GeV is the value of the quark mass from the analysis of the static characteristics. The parameter $Q_0^2 \sim 4$ GeV$^2$ is chosen so that the well-established data on $F^{\pi}(Q^2)$ at $Q^2 \leq 4$ GeV$^2$ can be described well by the theoretical curve. The decrease of the quark mass with growing $Q^2$ results in broadening of $\exp\left\{-\frac{m^2}{2\Lambda^2 x(1-x)}\right\}$ distribution at $x \to 1$ therefore the formfactor falls off slower as $q_\perp^2$ grows (Fig.3, dashed curve), e.g. at $q_\perp^2 \simeq 10$ GeV$^2$ the quantity $F_\pi(Q^2)$ increases approximately 1.5 times as compared to the constant mass case. All the further results will be given for the variable mass case (27).

As was already mentioned, the $q_\perp^2$ dependence in (26) is strongly weakened. This means that characteristic distances in hadrons decrease very slowly with increasing $q_\perp^2$, and fall off only twice at $q_\perp^2 \sim 10$ GeV$^2$ as compared to $q_\perp^2 \sim 0$. If we take for estimates the following value of constituent quark radius $\langle r_q^2 \rangle \sim 0{,}1 \langle R_h^2 \rangle \sim 1$ Fm$^2$, then at $Q^2 \gtrsim 5$-$10$ GeV$^2$ the wave functions of the quarks must overlap, and these values of $Q^2$ determine the range of validity of the considered model.

It is interesting to compare the contribution of (26) into pion formfactor with that of the perturbative QCD asymptotic formula. They become equal at $Q^2 \sim 40$ GeV$^2$ (in the case of $m = \text{const}$ at $Q^2 \sim 20$ GeV$^2$). However this estimate should be regarded as a very rough one. On the one hand, the behaviour of formfactor (26) at large $Q^2$ is sensitive both to the dependence of $m(Q^2)$ on $Q^2$ and to the behaviour of the vertex function at $x \to 1$, which is not fixed by the description of the static characteristics; besides, there is an additional uncertainty due to the account of the Sudakov formfactor. On the other hand, this estimate is beyond the range of validity of the model and in this region of $Q^2$ other interaction mechanisms connected with the overlapping of the constituent quark wave

functions may possibly be involved.

2) Formfactors of $\rho$-meson. The electromagnetic current of $\rho$-meson has the form:

$$<P',\lambda'|J_\mu|P\lambda> = e^{\lambda'}_\beta(P')\,e^{\lambda}_\alpha(P)\Big[-g_{\alpha\beta}(P+P')_\mu F_1(Q^2) + \\ +(g_{\mu\alpha}q_\beta - g_{\mu\beta}q_\alpha)\big[F_1(Q^2)+F_2(Q^2)\big] + q_\alpha q_\beta (P+P')_\mu F_3(Q^2)/m^2_\rho \tag{28}$$

where $q = P-P'$, $e^{\lambda}(P)$ is the polarization vector of the $\rho$-meson, $F_1(Q^2)$ is the electric formfactor. Formfactors $F_2(Q^2)$ and $F_3(Q^2)$ are related to magnetic and quadrupole moments as follows (see, e.g. [13]):

$$\mu = 1 + F_2(0)$$
$$\mathcal{D} = \frac{1}{m_\rho}\left(F_2(0) - 2F_3(0)\right) \tag{29}$$

Remind, that when calculating in the RQM the matrix elements of the type of $<P',\lambda'|J_\mu|P,\lambda>$, it is necessary to use the "good" components of electromagnetic current ( $J_0$ or $J_3$ ) [5,6]. Besides, it is undesirable to use the longitudinal polarization of vector mesons, since in this case the polarization vectors depend on the meson mass and an uncertainty due to mass defect in the quarks-meson vertex arises in calculations. Therefore in calculating formfactor $F_2^\rho(Q^2)$ one has, unfortunately, to apply the transverse component of current $J_1$, and in this case the vacuum fluctuations may be present, so the result for $F_2^\rho(Q^2)$ should be regarded less trustworthy. We have obtained the following expressions for the formfactors $F_i^\rho(Q^2)$.

$$F_1(Q^2) = \frac{N^2}{16\pi\Lambda^4}\int \frac{dx_1\,d^2\kappa_\perp}{x_1^2x_2^2(\epsilon_1+m)(\epsilon_2+m)}\exp\left\{-\frac{\kappa_\perp^2+m^2+q_\perp^2x_2^2/4}{2\Lambda^2x_1x_2}\right\}\times \tag{30}$$
$$\times\left\{\left[m^2+\kappa_\perp^2-\frac{q_\perp^2x_2^2}{4}\right](\epsilon_1+m)(\epsilon_2+m)+\left(\kappa_\perp^2-\frac{(\vec{\kappa}_\perp\vec{q}_\perp)^2}{q_\perp^2}\right)\left[2x_1x_2(\epsilon_1-\epsilon_2)^2-\frac{x_2^2q_\perp^2}{2}\right]\right\}$$

$$F_2(Q^2)=\frac{N^2}{16\pi\Lambda^4}\int\frac{dx_1\,d^2\kappa_\perp}{x_1^2x_2(\epsilon_1+m)(\epsilon_2+m)}\exp\left\{-\frac{\kappa_\perp^2+m^2+\frac{q_\perp^2x_2^2}{4}}{2\Lambda^2x_1x_2}\right\}\times$$

$$\times\left\{\frac{(\epsilon_1+m)(\epsilon_2+m)}{x_1}\left[\kappa_\perp^2+m^2+\frac{x_2^2q_\perp^2}{4}-\frac{2(\vec\kappa_\perp\vec q_\perp)^2}{q_\perp^2}\right]+\right. \tag{31}$$

$$+\frac{m(\epsilon_1+m)}{x_1}\left(\frac{x_1x_2q_\perp^2}{2}+\frac{2(\kappa_\perp q_\perp)^2}{q_\perp^2}+\frac{(\epsilon_1-\epsilon_2)\kappa_\perp q_\perp\cdot m}{2x_1}+\right.$$

$$\left.\left.+\left(\kappa_\perp^2-\frac{(\kappa_\perp q_\perp)^2}{q_\perp^2}\right)\left[2(x_2-x_1)(\epsilon_1-\epsilon_2)^2+x_2q_\perp^2\right]\right\}\right.$$

$$F_3(Q^2)=\frac{N^2m^2\rho}{16\pi\Lambda^4q_\perp^2}\int\frac{dx_1\,d^2\kappa_\perp}{x_1^2x_2^2(\epsilon_1+m)(\epsilon_2+m)}\exp\left\{-\frac{\kappa_\perp^2+m^2+q_\perp^2x_2^2/4}{2\Lambda^2x_1x_2}\right\}\times \tag{32}$$

$$\times\left\{\left(\kappa_\perp^2+\frac{q_\perp^2x_2^2}{4}-\frac{2(\vec\kappa_\perp\vec q_\perp)^2}{q_\perp^2}\right)\left(\frac{x_2^2q_\perp^2}{2}-2x_1x_2(\epsilon_1-\epsilon_2)^2\right)+\right.$$

$$\left.+m(\epsilon_1-\epsilon_2)\cdot(\kappa_\perp q_\perp)\cdot x_2+m(\epsilon_1+m)q_\perp^2x_2^2\right\}$$

Here and hereafter $\epsilon_i=\sqrt{\kappa_i^2+m^2}$ , where $\vec\kappa_{1\perp}=\vec\kappa_\perp+\frac{x_2\vec q_\perp}{2}$ , $\vec\kappa_{2\perp}=\vec\kappa_\perp-\frac{x_2\vec q_\perp}{2}$ , $x_2=1-x_1$ . The results are given in Fig.4. It is interesting that $F_1\simeq F^{\pi}$ with a good accuracy, and $F_2(Q^2)$ coincides up to $Q^2\sim 5$ GeV$^2$ with the VDM prediction. In the region $Q^2$ = 1-3 GeV$^2$ our results are qualitatively close to the predictions of DSR [13]; however quantitatively they exceed them 2-2.5 times. Our obtained values of the magnetic and quadrupole moments

$$\mu=2{,}3\ ;\qquad \mathcal{D}=\frac{0{,}45}{m^2\rho} \tag{33}$$

are close to the predictions of [13]. The electromagnetic radii corresponding to the formfactors $F_i^{\rho}(Q^2)$ are

$$\langle r_{F_1}^2\rangle=11.2\ \text{GeV}^{-2},\quad \langle r_{F_2}^2\rangle=9.9\ \text{GeV}^{-2},\quad \langle r_{F_3}^2\rangle=13.9\ \text{GeV}^{-2} \tag{34}$$

In order to compare our results with the asymptotic formulae of the QCD perturbation theory, it is convenient to use instead of formfactors $F_1$, $F_2$ and $F_3$ the helicity amplitudes in the Breit frame:

$$F_{TT}(Q^2) = \langle P', \lambda_T | J_0 | P, \lambda_T \rangle / 2E = F_1(Q^2)$$

$$F_{LT}(Q^2) = \langle P', \lambda_L | J_\perp | P, \lambda_T \rangle / 2E = \frac{Q}{2m_\rho} [F_1(Q^2) + F_2(Q^2)] \tag{35}$$

$$F_{LL}(Q^2) = \langle P', \lambda_L | J_0 | P, \lambda_L \rangle / 2E = F_1(Q^2) - \frac{Q^2}{2m_\rho} F_2(Q^2) + \frac{Q^2}{m_\rho^2}\left(1 + \frac{Q^2}{4m_\rho^2}\right) F_3(Q^2)$$

where $2E = \sqrt{Q^2 + 4m_\rho^2}$, $\lambda_T$ and $\lambda_L$ denote transverse and longitudinal polarizations of $\rho$-meson. In QCD perturbation theory $F_{LL} \sim -\frac{1}{Q^2}$ [9], $F_{LT} \sim \frac{1}{Q^3}$, $F_{TT} \sim \frac{1}{Q^4}$ [19]. As is seen from the Figure, our results are close qualitatively to the DSR predictions [13] and differ strongly from the asymptotic formulae of QCD.

3) Formfactors of $A_1$-meson. Electromagnetic current of $A_1$-mesons has the form of (28). Having done calculations by analogy with the $\rho$-meson case we obtain the following expressions for the formfactors

$$F_1(Q^2) = \frac{N_A^2}{8\Lambda^2} \int dx_1 \left\{ (x_1^2 + x_2^2) 2\Lambda^2 + \frac{m^2(x_1 - x_2)^2 - q_\perp^2 x_2^2}{x_1 x_2} \right\} \exp\left\{ - \frac{m^2 + \frac{q_\perp^2 x_2^2}{4}}{2\Lambda^2 x_1 x_2} \right\} \tag{36}$$

$$F_2(Q^2) = \frac{N_A^2}{8\Lambda^2} \int \frac{x_2 dx_1}{x_1} \left\{ \frac{m^2(x_1 - x_2)^2 + 4\Lambda^2 (x_1 - x_2) x_1^2 x_2 + q_\perp^2 x_2^2}{x_1 x_2} \right\} \exp\left\{ - \frac{m^2 + \frac{q_\perp^2 x_2^2}{4}}{2\Lambda^2 x_1 x_2} \right\} \tag{37}$$

$$F_3(Q^2) = \frac{N_A^2 M_A^2}{8\Lambda^2} \int x_2^2 dx_1 \exp\left\{ - \frac{m^2 + \frac{q_\perp^2 x_2^2}{4}}{2\Lambda^2 x_1 x_2} \right\} \tag{38}$$

As one can see from Fig.6, in the region $Q^2 = 0.5\text{-}3\ \text{GeV}^2$ our results agree well with the DSR predictions [13]. The essential difference between the $A_1$-meson formfactors and the corresponding ones of the $\rho$-meson should be mentioned. The formfactors $F_1^A$ and $F_2^A$ fall off much more rapidly with increasing $q_\perp^2$ than $F_1^\rho$ and $F_2^\rho$ do; $F_3^{A_1}$ falls off slower exceeding $F_1^{A_1}$ and $F_2^{A_1}$ in the whole region as distinct from the $\rho$-meson case. The magnetic and quadrupole moments of $A_1$-meson are respectively

$$\mu_{A_1} = 1{,}7 \quad , \quad \mathcal{D}_{A_1} = -5{,}1\,\frac{1}{m_{A_1}^2} \tag{39}$$

Note, that $\mathcal{D}_{A_1} \gg \mathcal{D}_\rho$ according to the fact that $A_1$-meson is a bound state with a nonzero angular orbital momentum $\ell = 1$.

Emphasize the following fact. Even at small $Q^2$ the behaviour of formfactors $F_1^{A_1}(Q^2)$ and $F_2^{A_1}(Q^2)$ differs essentially from the VDM predictions: $F_1^{A_1}(Q^2)$ falls off very rapidly with the growth of $Q^2$, and $F_2^{A_1}(Q^2)$ has a maximum at $Q^2 \sim 0.1\ \text{GeV}^2$. Electromagnetic radii corresponding to $F_i^{A_2}(Q^2)$ are $\langle r_{F_1}^2 \rangle = 17\ \text{GeV}^{-2}$, $\langle r_{F_2}^2 \rangle = -5\ \text{GeV}^{-2}$, $\langle r_{F_3}^2 \rangle = 11\ \text{GeV}^{-2}$, whereas $\langle r_{VDM}^2 \rangle = 10\ \text{GeV}^{-2}$.

## 4. Formfactors of $\omega \to \pi\gamma$ and $A_1 \to \pi\gamma$ Transitions

The formfactors of the $\omega \to \pi\gamma$ and $A_1 \to \pi\gamma$ transitions are defined, respectively, in the following way

$$\langle \pi(P') | J_\mu | \omega(P,\lambda) \rangle = G_{\omega\pi}(Q^2)\, \epsilon_{\mu\nu\alpha\beta}\, e_\nu^\lambda(P)\, P'_\alpha\, P_\beta \tag{40}$$

$$\langle \pi(P') | J_\mu | A_1(P,\lambda) \rangle = \frac{1}{M_{A_1}} \Big\{ [P_\eta g_{\lambda\sigma} - P_\lambda q_\sigma] G_1(Q^2) + \frac{1}{M_A^2} [P_\eta q_\lambda - q^2 P_\lambda] q_\sigma G_2(Q^2) \Big\}\, e_\sigma^\lambda(P) \tag{41}$$

where $\mathcal{P} = P + P'$

Having calculated in a standard way we obtain for $G_{\omega\pi}(Q^2)$ the following expression

$$G_{\omega\pi}(Q^2) = \frac{N^2}{8\pi\Lambda^4}\int\frac{dx_1 d^2k_\perp}{x_1^2 x_2}\left\{\frac{k_\perp^2 - (\vec{k}_\perp\vec{q}_\perp)^2/q_\perp^2}{\epsilon_1 + m} + m\right\}\exp\left\{-\frac{k_\perp^2 + m^2 + \frac{q_\perp^2 x_2^2}{4}}{2\Lambda^2 x_1 x_2}\right\} \quad (42)$$

$$G_{\omega\pi}(0) = 2{,}25\ \text{ГэВ}^{-1}$$

The width of the $\omega \to \pi\gamma$ decay has the form:

$$\Gamma_{\omega\pi} = \frac{G_{\omega\pi}^2(0)\alpha}{3}\left[\frac{M_\omega - M_\pi}{2M_\omega}\right]^3 \quad (43)$$

The account of anomalous magnetic moments of quarks [6] leads to an approximately 10% increase of the value of $G_{\omega\pi}(0)$. We obtain for the $\omega \to \pi\gamma$ width $\Gamma_{\omega\pi}$ = 826 keV ( $\Gamma_{\omega\pi}^{\text{эксп}}$ = 861±56 keV). $G_{\omega\pi}(Q^2)$ behaves approximately as the pion formfactor

$$G_{\omega\pi}(Q^2)/G_{\omega\pi}(0) \simeq F_\pi(Q^2) \quad (44)$$

and in the region $Q^2 \sim$ 1-3 GeV$^2$ is by about 30% lower than the predictions of both VDM and DSR [14].

In the case of $A_1 \to \pi\gamma$ transition, making use of the "good" components of current ( $J_0$, $J_3$ ) one can derive only a combination of formfactors

$$G_{A\pi}(Q^2) = \frac{G_1}{m_A} - \frac{G_2 q_\perp^2}{m_A^3} \quad (45)$$

To define the second formfactor (we choose $G_2$ ) we have, unfortunately, to use the transverse component of current $J_\perp$ ; in this case the contribution of vacuum fluctuations is possible, so the result depends on the direction of the boost into IMF and, generally speaking, contains a non-

physical pole at $q_\perp^2 = m_A^2 + m_\pi^2$

However in the calculations in the "symmetric" frame

$$P=\left(P+\frac{M^2}{2P},\ P\left(1-\frac{q_\perp^2}{8P^2}\right),\ -\frac{q_\perp}{2}\right)\quad P'=\left(P+\frac{M'^2}{2P},\ P\left(1-\frac{q_\perp^2}{8P^2}\right),\ \frac{q_\perp}{2}\right) \tag{46}$$

the non-physical pole is absent and the result for $G_2(Q^2)$ can be considered reasonable (although less reliable than $G_{A\pi}(Q^2)$ ). We have obtained the following expressions for the formfactors:

$$G_{A\pi}(Q^2)=\frac{mNN_A}{8\Lambda^2}\int\frac{dx_1}{x_1}(1-2x_1)\exp\left\{-\frac{m^2+\frac{q_\perp^2x_2^2}{4}}{2\Lambda^2x_1x_2}\right\} \tag{47}$$

$$G_{A\pi}(0)=0{,}36\ \text{ГэВ}^{-1}\ ,$$

$$\frac{G_2(Q^2)}{m_A^3}=\frac{mNN_A}{8\Lambda^2}\int\frac{dx_1}{x_1}\exp\left\{-\frac{m^2+\frac{q_\perp^2x_2^2}{4}}{2\Lambda^2x_1x_2}\right\}\frac{1}{m_A^2-m_\pi^2} \tag{48}$$

$$G_2(0)=2$$

In the region $Q^2\sim 1\text{-}3\ \text{GeV}^2$ our result (Fig.7) for $G_2(Q^2)$ agrees with the DSR predictions [13] within 15%. For the formfactor $G_1$ (and also $G_{A\pi}$ defined reliably in RQM) the predictions in the both approaches differ even qualitatively.

However one should keep in mind that as the authors mention [13], the DSR predictions have a semi-qualitative character (with the accuracy up to the factor of 1.5-2).

Note a non-trivial dependence of the formfactors $G_1(Q^2)$ and $G_{A\pi}(Q^2)$ on $Q^2$ . The formfactor $G_1(Q^2)$ has a pronounced minimum at $Q^2\sim$ $\sim$ 0.5 GeV$^2$, grows with increasing $Q^2$ up to $Q^2\sim 4$ GeV$^2$ and at further increase of $Q^2$ falls off very slowly. The formfactor $G_{A\pi}(Q^2)$ falls off rapidly as $Q^2$ increases and changes its sign at $Q^2\sim 0.5$ GeV$^2$.

The behaviour of these formfactors differs sharply from the VDM predictions even at small $Q^2$. The electromagnetic radii corresponding to these formfactors are: $\langle r^2_{G_1} \rangle \simeq 16$ GeV$^{-2}$, $\langle r^2_{G_{A\pi}} \rangle = 31$ GeV$^{-2}$. Formfactor $G_2(Q^2)$ falls off somewhat quicker, than that in the vector dominance model, and in the region $Q^2 \lesssim 2$ GeV$^2$ agrees with the VDM prediction within 20%, $\langle r^2_{G_2} \rangle = 12$ GeV$^2$.

The width of the $A_1 \to \pi\gamma$ decay is expressed via $G_{A\pi}(0)$ as follows:

$$\Gamma_{A\pi} = \frac{4\alpha}{3} G^2_{A\pi}(0) \left[ \frac{M_A^2 - m_\pi^2}{2M_A} \right]^3 \qquad (49)$$

thus being defined on the "good" components of the current. Our obtained width $\Gamma_{A\pi} = 319$ keV is nearly four times as less as existing at present experimental value $(\Gamma_{A\pi})_{\text{эксп}} = 1000$-$1500$ keV [20]. Emphasize, that at given $m$, $\Lambda_\pi$ the value $G_{A\pi}(0) = 2$ GeV$^{-1}$ is close to its possible maximum (taking $\Lambda_{A_1} \neq \Lambda_\pi$ we shall but diminish the width $\Gamma_{A\pi}$). Note in this connection, that under the same assumptions the width of the $B \to \pi\gamma$ decay, which is measured much more better, is in good agreement with the experiment *). Therefore it is natural to assume that the measured value of $A_1 \to \pi\gamma$ decay width is somewhat larger than needed.

Making use of the vector dominance model one can, in principle, estimate the $A_1 \to \rho\pi$ decay width. Here also one obtains too low value of $\Gamma_{A_1 \to \rho\pi}$. However, as was mentioned above, the validity of VDM at least for formfactor $G_1(Q^2)$ is somewhat doubtful, therefore such divergence should not be taken too seriously.

---

*) The authors are indebted to I.G.Aznauryan for this remark.

Results

In the relativistic quark model the structure of the pion wave function is investigated and the predictions for the formfactors of $\pi$ , $\rho$ , $A_1$ - mesons and those of $\omega \to \pi\gamma$ and $A_1 \to \pi\gamma$ transitions in the region $0 \lesssim Q^2 \lesssim 8$ GeV$^2$ are obtained.

It is shown that the axial projection of the pion low-energy wave function is close to the asymptotic wave function $\varphi_A^{ac}(x)$ , the tensor projection is much wider, and the pseudoscalar one is much narrower than $\varphi_A^{ac}(x)$ .

The available data on pion formfactor are described well on the basis of a simple quark diagram without gluon exchanges. The contribution of the perturbative QCD in the region $Q^2 \sim 5$ GeV$^2$ does not exceed 30%. Our results on the formfactors of $\pi$ and $A_1$ -mesons and on the $G_2(Q^2)$ formfactor of the $A_1 \to \pi\gamma$ transition in the region $Q^2 \approx$ 1-3 GeV$^2$ agree well with the DSR predictions. The $\rho$ -meson formfactors are in rough qualitative agreement with the DSR results and exceed them approximately by a factor of two. The results for the formfactor of $\omega \to \pi\gamma$ transition are in agreement in the both approaches within 30%.

In the framework of the model the meson formfactors depend essentially on its quantum numbers. For the $S$ -wave bound states the behaviour of the formfactors is smooth and does not differ much from the VDM predictions.

The "scaling" law .

$$F_1^\rho(Q^2) \simeq F^\pi(Q^2) \simeq G_{\omega\pi}(Q^2)/G_{\omega\pi}(0)$$

holds approximately. The $F_2^\rho(Q^2)$ formfactor falls off somewhat slower, the $F_3^\rho(Q^2)$ one - more rapidly as compared with $F_1^\rho(Q^2)$. For the $P$ -wave bound states the dependence of the formfactors on $Q^2$ is non-

trivial and cannot be described by VDM even at small $Q^2$ . Thus, $F_2^A(Q^2)$ has a maximum at $Q^2 \sim 0.1$ GeV$^2$, and its corresponding mean-square radius is negative. The $G_1(Q^2)$ formfactor of the $A_1 \to \pi\gamma$ transition has a minimum at $Q^2 \simeq 0.5$ GeV$^2$ and grows with increasing $Q^2$ in the region $0.5 \leqslant Q^2 \lesssim 4$ GeV$^2$.

The authors are thankful to I.G.Aznauryan for the useful discussions.

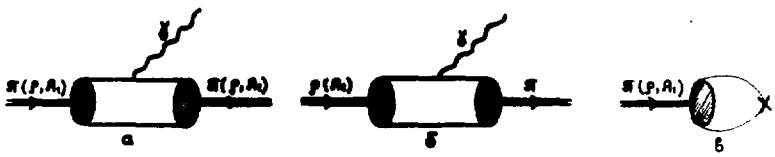


Fig.1

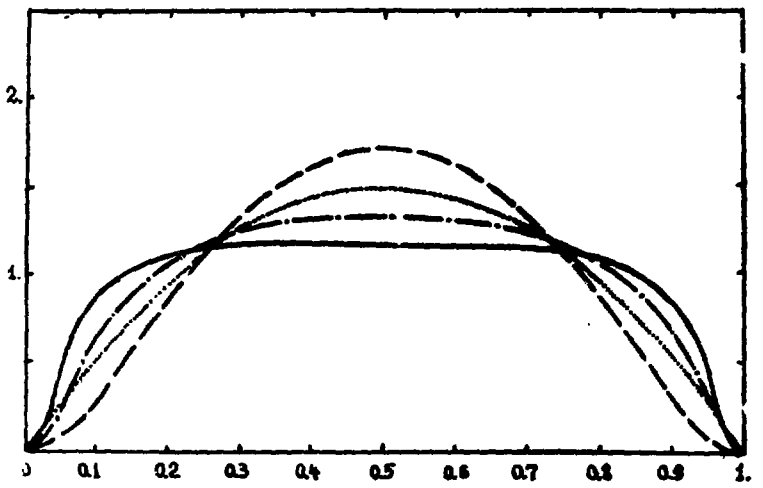


Fig.2

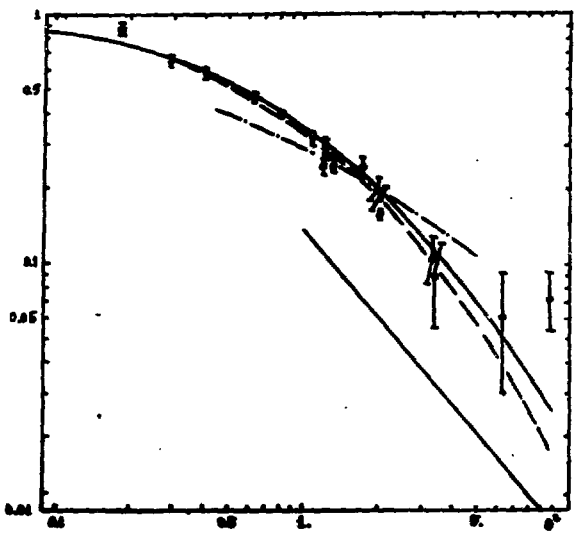

Fig.3

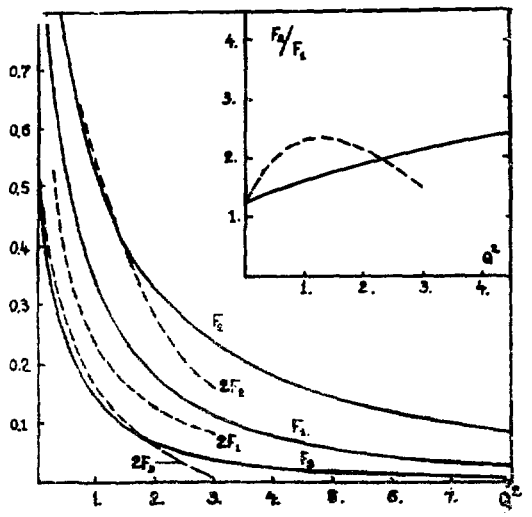
0.7
0.6
0.5
0.4
0.3
0.2
0.1
1.
2.
3.
4.
5.
6.
7.
$Q^2$
$F_2$
$2F_2$
$F_L$
$2F_L$
$F_3$
$2F_3$
$F_3/F_L$
4.
3.
2.
1.
$Q^2$
1.
2.
3.
4.

Fig.4

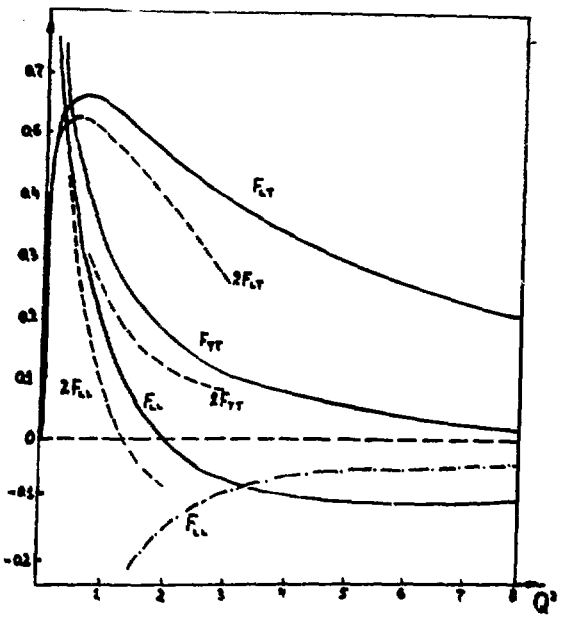
$F_{LT}$
$2F_{LT}$
$F_{TT}$
$2F_{TT}$
$2F_{LL}$
$F_{LL}$
$F_{LL}$
$Q^2$

Fig.5

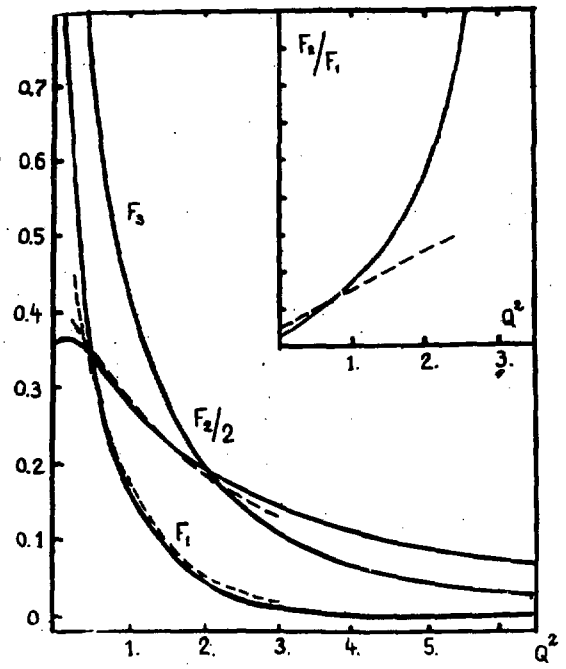
0.7
0.6
0.5
0.4
0.3
0.2
0.1
0
1.
2.
3.
4.
5.
$Q^2$
$F_3$
$F_2/2$
$F_1$
$F_3/F_1$
$Q^2$
1.
2.
3.

Fig.6

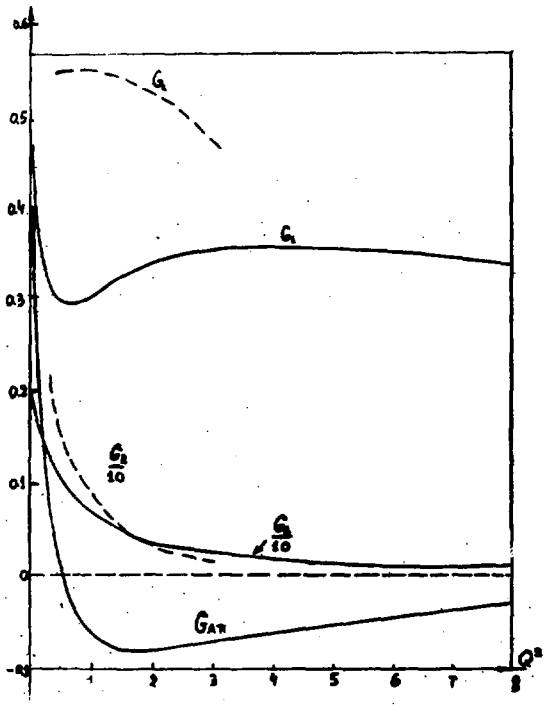
$G_1$
$G_2$
$\frac{G_2}{10}$
$\frac{G_3}{10}$
$G_{AN}$
$Q^2$

Fig.7

## Figure Captions

Fig.1. The old-fashioned perturbation theory diagrams determining the behaviour of formfactors of $\pi$ , $\rho$ , $A_1$ -mesons (a) and formfactors of the transitions $\omega(A_1) \to \pi\gamma$ (b); a diagram corresponding to constants $f_\rho$ , $f_\pi$ , $f_A$ (c). The cross denotes vector (axial) current.

Fig.2. Normalized pion wave functions $2\varphi_I(x)/f_I$ , $I = P, A, T$ in RQM. The pseudoscalar projection (solid curve), the axial projection (dash-dotted curve), the tensor projection (dashed curve). The asymptotic wave function (dotted curve) is given for comparison.

Fig.3. The pion electromagnetic formfactor in RQM. The dashed curve corresponds to the variable mass (27). For comparison are given the QCD DSR results [12] (dash-dotted curve) and the contribution of perturbative QCD (the lower straight line).

Fig.4. The $\rho$ -meson formfactor in RQM. The DSR results (dashed curves) are given for comparison.

Fig.5. The helicity formfactors of $\rho$ -meson in RQM (solid curves) and in DSR of QCD (dashed curves). The dash-dotted curve is the perturbative QCD contribution corresponding to the wave function ( $\varphi^L$ ).

Fig.6. The $A_1$ -meson formfactors in RQM (solid curves) and in DSR (dashed curves).

Fig.7. The $A_1 \to \pi\gamma$ transition formfactors in RQM (solid curves) and in DSR (dashed curves).

## REFERENCES


I. Вайнштейн А.И., Захаров В.Н., Новиков В.А., Ширман Н.А. Квантовая хромодинамика и физика резонансов. Элементарные частицы. Восьмая школа физиков ИТЭФ. М.:Энергоиздат вып.I, с.5-54. I980.

2. Терентьев М.В. Мезоны из релятивистских кварков. Препринт ИТЭФ-6, Москва, I976.

3. Терентьев М.В. О структуре волновых функций мезонов как связанных состояний релятивистских кварков. ЯФ, I976, т.24, с.207, 2I3.

4. Берестецкий В.Б., Терентьев М.В. Динамика светового фронта и нуклона из релятивистских кварков. ЯФ, I976, т.24, с.I044 -I057.

5. Aznauryan I.G., Bagdasaryan A.S., Ter-Isaakyan N.L. Relativistic Quark Model in the Infinite Momentum Frame and Static Properties of Nucleon.- Phys.Lett., 1982, v.112B, p.393.

6. Азнаурян И.Г., Багдасарян А.С., Тер-Исаакян Н.Л. Релятивистская модель кварков в системе бесконечного импульса и статические свойства нуклонов. ЯФ, I982, т.36, с.I276-I289.

7. Азнаурян И.Г., Багдасарян А.С., Тер-Исаакян К.Л. Магнитные моменты и лептонные распады октета барионов в релятивистской кварковой модели. ЯФ, I984, т.39, с.I08-II.

8. Aznauryan I.G., Bagdasaryan A.S., Ter-Isaakyan N.L. Relativistic Quark Model in Infinite Momentum Frame and Static Properties of Hadrons. - Preprint EPI-550(37)-82, Yerevan, 1982.

9. Багдасарян А.С., Есайбекян С.В., Тер-Исаакян Н.Л. Реляти-

вистская модель кварков и поведение электромагнитных форм-факторов мезонов в области малых и промежуточных $Q^2$ . ЯФ, 1983, т.38, с.402-410.

10. Терентьев М.В. Волновая функция мезона в квантовой хромодинамике и конституентной кварковой модели - попытка единого описания . ЯФ, 1983, т.38, с.213-225.

11. Nesterenko V.A., Radyushkin A.V. Sum Rules and Pion Form Factor in QCD.- Phys.Lett., 1982, v.115B, p.410.

12. Ioffe B.L., Smilga A.V. Pion Form-Factor at Intermediate Momentum Transfer in QCD. - Phys.Lett., 1982, v.114B, p.353.

13. Ioffe B.L., Smilga A.V. Meson Widths and Formfactors at Intermediate Momentum Transfer in Nonperturbative QCD. - Nucl.Phys., 1982, v.B216, p.373-407.

14. Eletsky V.L., Kogh Ya.I. Calculation of Electromagnetic Formfactor from QCD Sum Rules. - Preprint ITEP 170, 1982.

15. Reinders L.S., Rubinstein H.R., Yazake S. L=1 Light Quark Mesons in QCD. - Nucl.Phys., 1982, v.B196.

16. Черняк В.Л. Асимптотическое поведение эксклюзивных амплитуд в квантовой хромодинамике. Материалы XУ Зимней школы ЛИЯФ, Ленинград, 1980, с.65-154.

17. Chernyak V.L., Zhitnitsky A.R. Exclusive Decays of Heavy Mesons . - Nucl.Phys., 1982, v.B201, p.492-526.

18. Politzer H.D. Effective Quark Mass in the Chiral Limit. - Nucl.Phys., 1976, v.B117, p.397-406.

19. Vainshtein A.I., Zakharov V.I. Remarks on Electromagnetic Form Factors of Hadrons in the Quark Model. - Phys.Lett., 1977, v.72B, No.3

20. Hiltin D., Rapporteur Talk. Radiative Decays, Light Quark Spectroscopy and Glueball Searches Lepton-Proton Interactions, Cornell, 1983.

The manuscript was received 18 May 1984

А.О.БАГДАСАРЯН, С.В.ЕСАЙБЕГЯН, Н.Л.ТЕР-ИСААКЯН

ФОРМФАКТОРЫ МЕЗОНОВ И МЕЗОННЫХ РЕЗОНАНСОВ ПРИ МАЛЫХ И ПРОМЕЖУТОЧНЫХ ПЕРЕДАЧАХ $Q^2$ В РЕЛЯТИВИСТСКОЙ КВАРКОВОЙ МОДЕЛИ

(на английском языке, перевод Б.Н.Асланян)

Редактор Л.П.Мукаян

Технический редактор А.О.Абрамян

Подписано в печать 4/XII-84 Бч-10854 Формат 60х84/16
Офсетная печать. Уч.изд.л. 2.0 Тираж 299 экз. П.30 к.
Зак.тип.№ 910 Индекс 3624

Отпечатано в Ереванском физическом институте
Ереван 36, Маркаряна 2

индекс 3624

ЕРЕВАНСКИЙ ФИЗИЧЕСКИЙ ИНСТИТУТ